JOC*Article*

Theoretical Investigation of Lone Pair Inversions, Ring Openings, and Hydride Shifts in *O*-Methylated Epoxides

Jeffrey W. Schubert, Timothy J. Dudley, and Brian K. Ohta*

Department of Chemistry, 800 Lancaster Avenue, Villanova University, Villanova, Pennsylvania 19085

brian.ohta@villanova.edu

Received November 29, 2006

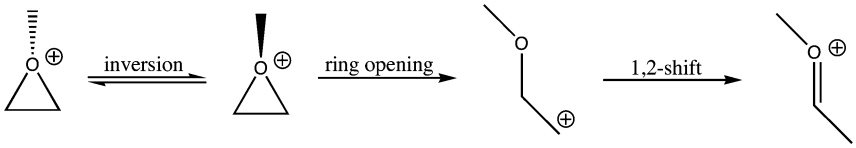

Mechanisms associated with the isomerization of the *O*-methylethylene oxonium ion and its tetramethyl-substituted analogue have been explored using correlated electronic structure calculations. The minima and transition states associated with inversion at the oxygen atom, as well as those associated with opening of the epoxide ring, have been characterized. The calculated barrier to inversion at the oxygen atom for the *O*-methylethylene oxonium ion, 15.7 kcal/mol, agrees well with the experimentally determined value, 10 ± 2 kcal/mol. Our calculations indicate that a significantly higher barrier exists for the ring-opening mechanism that leads to more thermodynamically stable structures. This work includes the first known calculations on the *O*-methyl-2,3-dimethyl-2-butene oxonium ion along with transition states and intermediates associated with ring opening and inversion at the oxygen atom. Results show that there is a significantly lower barrier to ring opening as compared to the *O*-methylethylene oxonium ion species, leading to a lower probability of isolating this species. The effects of basis sets and correlation techniques on these ions were also analyzed in this work. Our results indicate that the B3LYP/6-31G* level is reliable for obtaining molecular geometries for both minima and transition states on the $C_3H_7O^+$ and $C_7H_{15}O^+$ potential energy surfaces.

Introduction

Onium ions are an electron deficient species in which a hypervalent heteroatom bears a positive formal charge. The most famous examples of these species are cyclic 1,2-bridged halonium ions that were originally proposed over 70 years ago to explain stereospecific halogen addition to alkenes.[1] Since then, there have been numerous experimental and theoretical investigations into the structure, energetics, and reactivity of halonium ions.[2] In contrast to the intense attention given to 1,2-bridged halonium ions, there are few studies that address the analogous *O*-alkoxy-1,2-bridged oxonium ions even though oxonium ion salts are stable commercially available alkylating reagents.[3−6]

A focal point in the discussion of halonium ions has been the relative stability of the bridging species versus their corresponding classical halocarbenium ions.[7−10] Theoretical studies indicate that fluorine is the only halogen that cannot form a hypervalent bridge between carbon atoms and predict that the 1,2-bridged ethylene fluoronium ion will rearrange to a more stable 1-fluoroethyl cation.[9] Olah and Bollinger attempted to synthesize the tetramethylethylene fluoronium ion under superacidic conditions but instead produced the corresponding 1-fluorocarbenium ion.[11,12] To the authors' knowledge, there are no reports of a stable carbon-bridged fluoronium ion. Because oxygen and fluorine are similar with respect to the

* Corresponding author. Tel.: (610) 519-5324. Fax: (610) 519-7167.

(1) Roberts, I.; Kimball, G. E. *J. Am. Chem. Soc.* **1937**, *59*, 947−948.
(2) Olah, G. A. *Halonium Ions*; Wiley-Interscience: New York, 1975 and references therein.
(3) Renzi, G.; Roselli, G.; Grandinetti, F.; Filippi, A.; Speranza, M. *Angew. Chem., Int. Ed.* **2000**, *39*, 1673−1676.
(4) Nobes, R. H.; Radom, L. *Org. Mass. Spectrom.* **1984**, *19*, 385−393.
(5) Nobes, R. H.; Rodwell, W. R.; Bouma, W. J.; Radom, L. *J. Am. Chem. Soc.* **1981**, *103*, 1913−1922.
(6) Lambert, J. B.; Johnson, D. H. *J. Am. Chem. Soc.* **1968**, *90*, 1349−1350.
(7) Damrauer, R.; Leavell, M. D.; Hadad, C. M. *J. Org. Chem.* **1998**, *63*, 9476−9485.
(8) Rodriquez, C. F.; Bohme, D. K.; Hopkinson, A. C. *J. Am. Chem. Soc.* **1993**, *115*, 3263−3269.
(9) Reynolds, C. H. *J. Am. Chem. Soc.* **1992**, *114*, 8676−8682.
(10) Hamiltion, T. P.; Schaefer, H. F., III *J. Am. Chem. Soc.* **1990**, *112*, 8260−8265.
(11) Olah, G. A.; Bollinger, J. M. *J. Am. Chem. Soc.* **1967**, *89*, 4744−4752.
(12) Olah, G. A.; Prakash, G. K. S.; Krishnamurthy, V. V. *J. Org. Chem.* **1983**, *48*, 5116−5117.

10.1021/jo0624492 CCC: $37.00 © 2007 American Chemical Society
Published on Web 03/03/2007

factors that determine an atom's ability to form a hypervalent bridge, the analogous issue of the relative stabilities of *O*-alkyl-1,2-bridged oxonium ions and their corresponding alkoxycarbenium ions is worth examining.

Lambert and Johnson reported the direct formation and NMR characterization of *O*-alkoxy-1,2-bridged oxonium ions.[6] Trapping methyl cations with ethylene oxide at low temperatures generated the *O*-methylethylene oxonium ion. The epoxide ring protons appeared as an AA′BB′ spin system, which indicated that the *O*-methyl group does not traverse the σ_v plane of the epoxide on the NMR time scale. At higher temperatures, the signals coalesced with an activation barrier of 10 ± 2 kcal/mol. The barrier was ascribed to lone pair inversion on the oxygen; however, either C−C or C−O bond rotations in the 2-alkoxyethyl cation could be used to explain these results.

While numerous theoretical studies of protonated epoxides are known,[4,13−17] few studies involving methylated epoxides are reported.[3−6] Nobes and Radom[4] calculated the thermal stability of the *O*-methylethylene oxonium ion relative to other isomers of $C_3H_7O^+$. Using HF/3-21G and MP3/6-31G* calculations, they estimated that the 1,2-bridged oxonium ion is 30 kcal/mol lower in energy as compared with the open 2-methoxyethyl cation. They concluded that the open cation would undergo a barrierless 1,2-hydride shift to give the 1-methoxyethyl cation. They also concluded that hydride shifts prevent the formation of 1,2-bridged oxonium ions from other possible $C_3H_7O^+$-isomers. While this work focused on locating a large number of minima on the $C_3H_7O^+$ potential energy surface, as far as the authors are aware, no calculations have been reported on reaction pathways associated with the *O*-methylethylene oxonium ion.

In a recent paper, Carlier et al. examined a series of protonated epoxides and demonstrated that the geometries of some oxonium ions are sensitive to methods used for geometry optimization.[17] Specifically, the paper concludes that density functional methods applied to asymmetrically substituted oxonium ions will overestimate the C−O bond length on the more substituted carbon. They recommend MP2 or coupled cluster methods when examining asymmetric oxonium ions. More generally, they caution against the uncritical usage of B3LYP methods even though these methods are commonly applied to the transition states of asynchronous epoxidation reactions.[18−21] Because the transition state for C−O bond breaking in oxonium ions is intrinsically asymmetric, a critical examination of the effect of computational methodology on the geometries of oxonium ion transition state structures is prudent.

Considering the alternative processes to describe the *O*-methyl dynamics, our interest in the ability of oxygen to form a 1,2-bridged oxonium ion, and the possible limitation of density functional methods on asymmetric transition states, we report the relevant stationary points on the potential energy surface of oxonium ions using modern computational methods. The reaction pathways explored in this work are the inversion process for the *O*-methylethylene oxonium ion (Scheme 1) and the ring opening of this ion to form either *cis*- or *trans*-1-methoxyethyl cation (Scheme 2). A similar analysis will be performed on a substituted form of *O*-methylethylene oxonium ion in which the hydrogens on the ethylene fragment are replaced with methyl groups. The effects of substitution on structures and energetics of reaction intermediates will be analyzed.

SCHEME 1

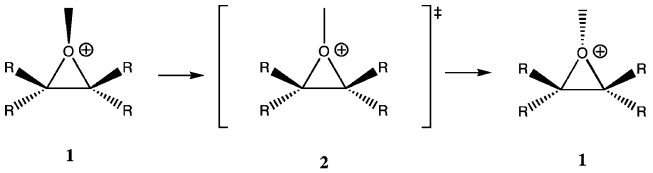

{R = H: **1H**,**2H**}
{R = Me: **1M**,**2M**}

SCHEME 2

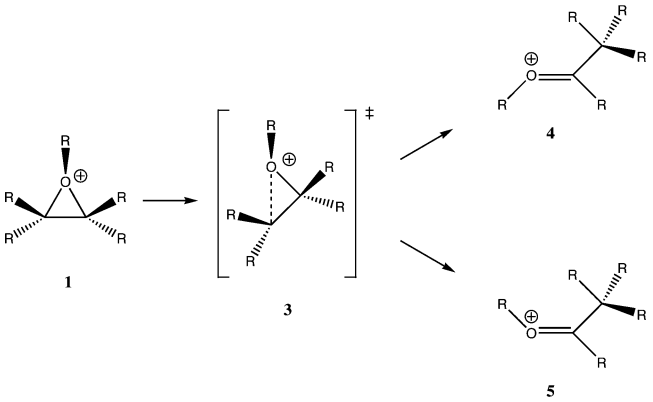

{R = H: **3H**-**5H**}
{R = Me: **3M**-**5M**}

Theoretical Calculations

For the $C_3H_7O^+$ series, geometries were optimized using second-order Møller−Plesset perturbation theory (MP2),[22] density functional theory, and CCSD(T).[23] The Becke 3-parameter exchange functional[24] was utilized in the DFT calculations with the Lee−Yang−Parr correlation functional,[25] commonly known as B3LYP. Two basis sets were utilized in the geometry optimizations: 6-31G*[26,27] and 6-311+G**.[28] Vibrational frequencies were calculated at all stationary points to determine whether each structure was an equilibrium structure or a transition state. Transition states

(13) Cremer, D.; Kraka, E. *J. Am. Chem. Soc.* **1985**, *107*, 3800−3810.
(14) Vila, A.; Mosquera, R. A. *Chem. Phys. Lett.* **2003**, *371*, 540−547.
(15) Ford, G. P.; Smith, C. T. *J. Am. Chem. Soc.* **1987**, *109*, 1325−1331.
(16) Na, J.; Houk, K. N.; Shevlin, C. G.; Janda, K. D.; Lerner, R. A. *J. Am. Chem. Soc.* **1993**, *115*, 8453−8454.
(17) Carlier, P. R.; Deora, N.; Crawford, T. D. *J. Org. Chem.* **2006**, *71*, 1592−1597.
(18) Bach, R. D.; Glukhovtsev, M. N.; Gonzalez, C.; Marquez, M.; Estévez, C. M.; Baboul, A. G; Schlegel, H. B. *J. Phys. Chem. A* **1997**, *101*, 6092−6100.
(19) Bach, R. D.; Dmitrenko, O. *J. Phys. Chem. A* **2003**, *107*, 4300−4306.
(20) Cheong, P. H. Y.; Yun, H.; Danishefsky, S. J.; Houk, K. N. *Org. Lett.* **2006**, *8*, 1513−1516.
(21) Singleton, D. A.; Wang, Z. *J. Am. Chem. Soc.* **2005**, *127*, 6679−6685.
(22) Head-Gordon, M.; Pople, J. A.; Frisch, M. J. *Chem. Phys. Lett.* **1988**, *153*, 503−506.
(23) Pople, J. A.; Head-Gordon, M.; Raghavachari, K. *J. Chem. Phys.* **1987**, *87*, 5968−5975.
(24) Becke, A. *J. Chem. Phys.* **1993**, *98*, 5648−5652.
(25) Lee, C. T.; Yang, W. T.; Parr, R. G. *Phys. Rev. B: Condens. Matter* **1988**, *37*, 785−789.
(26) Ditchfield, R.; Hehre, W. J.; Pople, J. A. *J. Chem. Phys.* **1971**, *54*, 724−728.
(27) Hehre, W. J.; Ditchfield, R.; Pople, J. A. *J. Chem. Phys.* **1972**, *56*, 2257−2261.
(28) Krishnan, R.; Binkley, J. S.; Seeger, R.; Pople, J. A. *J. Chem. Phys.* **1980**, *72*, 650−654.

possessed a unique imaginary frequency. Relative electronic energies were calculated at all levels of theory previously mentioned. Relative energies were calculated at B3LYP/6-31G* optimized geometries at the B3LYP, MP2, and CCSD(T) levels with the cc-pVTZ[29] basis set to analyze their accuracy. Zero-point energies (ZPE) reported in this work were calculated at the B3LYP/6-31G* optimized geometries. Intrinsic reaction coordinate (IRC) calculations were used to connect the B3LYP/6-31G* optimized transition states to their corresponding minima.

Geometries of the $C_7H_{15}O^+$ structures were optimized only at the B3LYP/6-31G* level based on the performance of such calculations for the $C_3H_7O^+$ series (*vide infra*). IRC calculations and ZPE corrections were also performed at the B3LYP/6-31G* level of theory. Relative energies were obtained at the MP2/cc-pVTZ//B3LYP/6-31G* level. All DFT and MP2 single-point energy calculations, geometry optimizations, and vibrational analyses were performed using the Spartan'04 computational chemistry software package[30] with default gradient tolerances. IRC and CCSD(T)[31] single-point calculations were performed using the GAMESS[32] electronic structure code. The second-order Gonzalez−Schlegel algorithm[33] was used in the IRC calculations with a step size of 0.30 (amu)$^{1/2}$ b. Only valence electrons were correlated in both MP2 and CCSD(T) calculations. GAMESS output was visualized using the MacMolPlt program.[34] CCSD(T) geometry optimizations and frequency calculations were performed using the Gaussian98 program.[35] Atomic charges based on the electrostatic model were obtained from the B3LYP/6-31G* optimized geometries in Spartan'04, with the hydrogen charges summed into the heavy atom charges.

Results

$C_3H_7O^+$. Recent work by Carlier et al. has shown that oxonium ion equilibrium geometries predicted by theoretical methods can vary significantly depending on the method and/or basis set used.[17] Therefore, a thorough analysis of the effects of basis sets and methods used in studying *O*-methyl oxonium ions is warranted. Figure 1 shows the structures of the two stationary points associated with Scheme 1 (**1H** and **2H**).

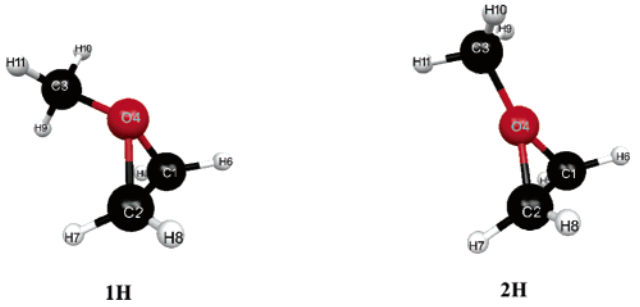

FIGURE 1. B3LYP/6-31G* geometries of *O*-methylethylene oxonium ion (**1H**) and the transition state associated with inversion at the oxygen atom (**2H**).

TABLE 1. Geometrical Parameters Determined for Structures 1H and 2H Using the 6-31G* Basis Set[a]

	C_1-C_2	C_2-O	$O-C_3$	C_2-O-C_3	$C_1-C_2-O-C_3$
1H (B3LYP)	1.467	1.505	1.487	119.9	108.7
1H (MP2)	1.464	1.505	1.491	118.0	107.2
1H (CCSD(T))	1.470	1.509	1.492	118.1	107.3
2H (B3LYP)	1.499	1.455	1.489	149.8	180.0
2H (MP2)	1.496	1.455	1.494	150.0	180.0
2H (CCSD(T))	1.502	1.458	1.495	149.8	180.0

[a] Bond lengths are given in angstroms, and bond and dihedral angles are given in degrees.

TABLE 2. Geometrical Parameters Determined for Structures 1H and 2H Using the 6-311+G Basis Set**[a]

	C_1-C_2	C_2-O	$O-C_3$	C_2-O-C_3	$C_1-C_2-O-C_3$
1H (B3LYP)	1.465	1.503	1.489	120.3	109.0
1H (MP2)	1.466	1.499	1.485	118.0	107.4
1H (CCSD(T))	1.469	1.493	1.482	118.8	108.1
2H (B3LYP)	1.495	1.456	1.500	148.2	180.0
2H (MP2)	1.498	1.449	1.493	147.8	180.0
2H (CCSD(T))	1.506	1.455	1.495	149.8	180.0

[a] Bond lengths are given in angstroms, and bond and dihedral angles are given in degrees.

Table 1 lists the geometrical parameters calculated for the *O*-methylethylene oxonium ion (**1H**) at the B3LYP, MP2, and CCSD(T) levels using the 6-31G* basis set. Table 1 also lists the geometrical parameters for the previously uncharacterized transition state corresponding to inversion of the substituents on the oxygen atom (**2H**). The data in Table 1 demonstrate that few differences are observed in the geometries optimized using different theories. Both the B3LYP and the MP2 geometries agree quite well with the CCSD(T) geometry for the small basis set. The only significant differences are the bond and dihedral angles at the B3LYP and MP2 levels, which differ between 0.1 and 1.8° from the CCSD(T) values for **1H**. For **2H**, the agreement between different theories is good as well, with the largest disagreement being underestimation of the $O-C_3$ bond length at the B3LYP level by 0.007 Å.

Table 2 lists a similar set of parameters evaluated using the 6-311+G** basis set. Larger differences between the B3LYP and MP2 results as compared to the CCSD(T) values are observed, particularly for the bond lengths. B3LYP overestimates the C_2-O bond length in **1H** by 0.010 Å and underestimates the C−C bond length in **2H** by 0.011 Å. All other bond lengths agree to within 0.010 Å. B3LYP also overestimates the C_2-O-C_3 angle by 1.5° in **1H** and underestimates the same bond angle by 1.6° in **2H**, with the MP2 bond angle in **2H** being 2.0° smaller. The effect of increasing basis set size on

(29) Dunning, T. H. *J. Chem. Phys.* **1989**, *90*, 1007−1023.
(30) *Spartan'04*; Wavefunction Inc.: Irvine, CA. Except for molecular mechanics and semi-empirical models, the calculation methods used in Spartan'04 have been documented in Kong, J.; White, C. A.; Krylov, A. I.; Sherrill, C. D.; Adamson, R. D.; Furlani, T. R.; Lee, M. S.; Lee, A. M.; Gwaltney, S. R.; Adams, T. R.; Ochsenfeld, C.; Gilbert, A. T. B.; Kedziora, G. S.; Rassolov, V. A.; Maurice, D. R.; Nair, N.; Shao, Y.; Beasley, N. A.; Maslen, P. E.; Dombroski, J. P.; Daschel, H.; Zhang, W.; Korambath, P. P.; Baker, J.; Byrd, E. F. C.; Van Voorhis, T.; Ouhi, M.; Hirata, S.; Hsu, C.-P.; Ishikawa, N.; Florian, J.; Warshel, A.; Johnson, B. G.; Gill, P. M. W.; Head-Gordon, M.; Pople, J. A. *J. Comput. Chem.* **2000**, *21*, 1532−1548.
(31) Piecuch, P.; Kucharski, S. A.; Kowalski, K.; Musial, M. *Comput. Phys. Commun.* **2002**, *149*, 71−96.
(32) Schmidt, M. W.; Baldridge, K. K.; Boatz, J. A.; Elbert, S. T.; Gordon, M. S.; Jensen, J. H.; Koseki, S.; Matsunaga, N.; Nguyen, K. A.; Su, S. J.; Windus, T. L.; Dupuis, M.; Montgomery, J. A. *J. Comput. Chem.* **1993**, *14*, 1347−1363.
(33) Gonzales, G.; Schlegel, H. B. *J. Chem. Phys.* **1989**, *90*, 2154−2161.
(34) Bode, B. M; Gordon, M. S. *J. Mol. Graphics Modell.* **1998**, *16*, 133−138.
(35) Frisch, M. J.; Trucks, G. W.; Schlegel, H. B.; Scuseria, G. E.; Robb, M. A.; Cheeseman, J. R.; Zakrzewski, V. G.; Montgomery, J. A.; Stratmaann, R. E.; Burant, J. C.; Dapprich, S.; Millam, J. M.; Daniels, A. D.; Kudin, K. N.; Strian, M. C.; Farkas, O.; Tomasi, J.; Barone, V.; Cossi, M.; Cammi, R.; Mennucci, B.; Pomelli, C.; Adamo, C.; Clifford, S.; Ochterski, J.; Peterson, G.A.; Ayala, P. Y.; Cui, Q.; Morokuma, K.; Malick, D. K.; Rabuck, A. D.; Raghavachari, K.; Foresman, J. B.; Cioslowski, J.; Ortiz, J. V.; Stefanov, B. B.; Liu, G.; Liashenko, A.; Piskorz, P.; Komaromi, I.; Gomperts, R.; Martin, R. L.; Fox, D. J.; Keith, T.; Al-Laham, M. A.; Peng, C. Y.; Nanayakkara, A.; Gonzalez, C.; Challacombe, M.; Gill, P. M. W.; Johnson, B. G.; Chen, W.; Wong, M. W.; Andres, J. L.; Head-Gordon, M.; Replogle, E. S.; Pople, J. A. *Gaussian 98*, revision A.1; Gaussian, Inc.: Pittsburgh, PA, 1998.

TABLE 3. Geometrical Parameters Determined for Structure 3H Using Various Theoretical Methods and Basis Sets[a]

	B3LYP		MP2		CCSD(T)	
	6-31G*	6-311+G**	6-31G*	6-311+G**	6-31G*	6-311+G**
C_1-C_2	1.452	1.449	1.448	1.452	1.455	1.460
C_2-O	1.402	1.404	1.406	1.401	1.402	1.398
$O-C_3$	1.438	1.440	1.447	1.441	1.450	1.444
C_1-C_2-O	103.8	102.7	103.0	102.8	105.1	104.9
C_2-O-C_3	116.3	116.7	114.0	113.9	114.6	114.3
$C_1-C_2-O-C_3$	105.4	105.6	99.0	99.3	104.6	104.4

[a] Bond lengths are given in angstroms, and bond and dihedral angles are given in degrees.

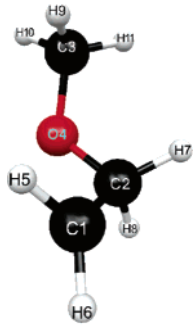

3H

FIGURE 2. B3LYP/6-31G* geometry of transition state associated with ring opening in **1H**.

the geometries of structures **1H** and **2H** appear to be minimal. Figure 2 shows the structure of another previously uncharacterized transition state that corresponds to opening of the ring through cleavage of a carbon−oxygen bond (**3H**).

Table 3 lists the geometrical parameters of **3H** calculated using various theoretical methods and basis sets. Cleavage of one of the carbon−oxygen bonds in the C−O−C ring is accompanied by a significant shortening of the other C−O bond (≈0.10 Å), suggesting the formation of a carbon−oxygen multiple bond and hydride shift.

The other bond lengths are seen to decrease as well, but to a lesser extent (<0.05 Å). As shown for structures **1H** and **2H**, excellent agreement is seen between geometries calculated at the B3LYP and MP2 levels regardless of the basis set used in this study. The one exception is the dihedral angle formed by the heavy atoms, which is predicted to be about 6° smaller at the MP2 level as compared to the corresponding value determined at the B3LYP level. The B3LYP and MP2 geometries agree well with the corresponding CCSD(T) geometries, with the exception of the MP2 dihedral angle being about 5° smaller. Notwithstanding the foregoing small geometric differences, the structural data in Tables 1−3 indicate that there is little dependence of the geometries of both minima and transition states on either the basis set or the method used. Thus, it is reasonable to assume that the B3LYP/6-31G* level is appropriate for obtaining geometries of cations of similar structure. From this point forward, unless otherwise noted, geometries reported are based on calculations at the B3LYP/6-31G* level.

Opening of the C−O−C ring in the *O*-methylethylene oxonium ion can lead to formation of one of two products: the *trans*- or *cis*-1-methoxyethyl cation (structures **4H** and **5H** in Figure 3, respectively). Table 4 lists the geometrical parameters calculated for these two species, along with the transition state associated with their interconversion (**6H**, Figure 3). The differences observed for the bond lengths in **4H** and **5H** are small as expected (≤0.005 Å), with larger deviations seen for the transition state structure, particularly for the carbon−oxygen double bond (≈0.020 Å decrease). The differences in the bond angles also show the expected trend, with the C_2-C_1-O bond angle being slightly larger for the cis-isomer due to steric effects.

Figure 4 is a potential energy diagram of the region of the $C_3H_7O^+$ potential energy surface characterized in this work. IRC calculations confirm that structure **2H** is the transition state associated with inversion of structure **1H** at the oxygen atom. While both structures exhibit C_s symmetry, the mirror plane in **1H** bisects the C−O−C angle in the ring, while the mirror plane in **2H** contains all carbon and oxygen atoms. Thus, the motion away from **2H** to form **1H** involves not only undulation of the heavy atoms but also rotation of the free methyl group. Structure **3H** was determined to be a transition state connecting structures **1H** and **4H**. The reaction coordinate leading from **3H** to **1H** was found to be relatively straightforward: formation of a C−O bond to form the C−O−C ring with rotation of the free methyl group on the oxygen atom. The reaction coordinate leading in the opposite direction was much more complex, involving rotation of the carbon−carbon bond in the ethylene fragment accompanied by a hydride shift. This species was previously characterized theoretically by Radom and Nobes at the HF/3-21G level,[4] but this minimum could not be isolated using correlated methods. IRC calculations connecting structure **6H** to the *cis*- and *trans*-1-methoxyethyl cations indicate that the reaction coordinate involves a simple C−O−C bend that maintains the planarity of the carbon and oxygen atoms.

Table 5 lists the relative energies of structures **1H**−**6H** calculated at various levels of theory and different basis sets. One can see that the effect of the basis set size is surprisingly small for the B3LYP, MP2, and CCSD(T) energy calculations. All levels of theory predict the same relative positions of the stationary points on the potential energy surface. The *O*-methylethylene oxonium ion (**1H**) is the highest energy minimum considered, and the *trans*- and *cis*-1-methoxyethyl cations (**4H** and **5H**) are lower energy minima, with the *trans*-isomer being slightly lower in energy (≈2.0−2.5 kcal/mol). The ring-opening transition state is predicted to be higher in energy than the *O*-inversion transition state at all levels of theory, but there is a large difference in the quantitative energy difference depending on the level of theory used. For most structures, MP2 energies agree quite well with the CCSD(T)/cc-pVTZ energies. The one exception is structure **3H**, where the relative energy is overestimated by about 5−7 kcal/mol depending on the basis set used. B3LYP energies differ significantly from the CCSD(T)/cc-pVTZ values for all structures. Since CCSD(T) calculations were too computationally demanding for the methylated species, they were not performed on the larger species considered in this work. MP2/cc-pVTZ calculations were used to

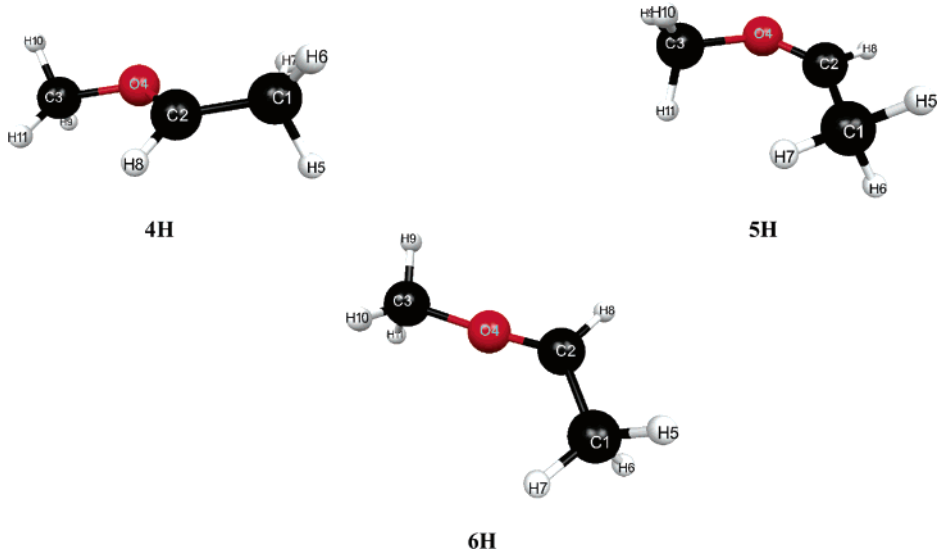

FIGURE 3. B3LYP/6-31G* geometries of *trans*- and *cis*-1-methoxyethyl cation (**4H** and **5H**, respectively) and the transition state (**6H**) associated with isomerization of **4H** and **5H**.

TABLE 4. Geometrical Parameters Determined for Structures 4H, 5H, and 6H at the B3LYP/6-31G* Level[a]

	C_1-C_2	C_2-O	$O-C_3$	C_1-C_2-O	C_2-O-C_3	$C_1-C_2-O-C_3$
4H	1.462	1.257	1.479	120.6	122.6	180.0
5H	1.465	1.259	1.484	127.9	124.2	0.0
6H	1.470	1.239	1.469	123.8	171.5	87.2

[a] Bond lengths are given in angstroms, and bond and dihedral angles are given in degrees.

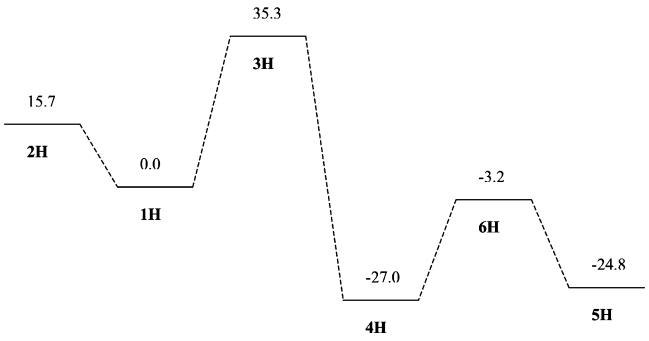

FIGURE 4. Potential energy diagram of the stationary points on the $C_3H_7O^+$ potential energy surface determined at the CCSD(T)/cc-pVTZ//B3LYP/6-31G* level. Relative energies are in kcal/mol and are not ZPE corrected.

predict the relative energies of these species based on the success of calculating relative energies for the $C_3H_7O^+$ series.

$C_7H_{15}O^+$. To the authors' knowledge, no previous theoretical work has been reported on the methylated analogues of **1H**−**4H**. Figure 5 shows the structures for tetramethylated structures (**1M** and **2M**) depicted in Scheme 1. Both structures have a plane of symmetry that bisects the epoxide ring. Table 6 lists the geometrical parameters determined for these structures at the B3LYP/6-31G* level of theory.

The structure of the transition state (**3M**) associated with the ring opening of **1M** is shown in Figure 6. IRC calculations were used to connect this transition state to structure **1M** and to a ring-opened intermediate (**7**), also shown in Figure 6. This intermediate is analogous to the intermediate on the $C_3H_7O^+$ potential energy surface that could only be obtained at the HF level. IRC calculations show that the motion leading from **3M** back to **1M** corresponds to closure of the C_1-O-C_2 ring as well as a rotation of the methyl group on the oxygen atom. The reaction coordinate leading to the open intermediate is a simple rotation of the C_1-C_2 bond. This reaction coordinate associated with **3M** differs from that for **3H** in that motion toward the open minimum does not include a methyl shift from C_1 to C_2.

TABLE 5. Relative Energies of Structures 1H−6H Calculated at Various Levels of Theory[a]

	1H	**2H**	**3H**	**4H**	**5H**	**6H**
B3LYP/6-31G*	0	13.0	29.4	−29.7	−27.2	−8.8
B3LYP/6-311+G**	0	12.3	27.5	−30.9	−28.3	−10.4
MP2/6-31G*	0	15.9	41.9	−25.3	−23.0	−1.9
MP2/6-311+G**	0	15.3	40.4	−26.4	−23.9	−2.5
CCSD(T)/6-31G*	0	16.0	35.8	−26.7	−24.4	−2.9
CCSD(T)/6-311+G**	0	15.3	34.7	−27.5	−25.1	−3.5
B3LYP/cc-pVTZ[b]	0	12.9	28.2	−30.7	−28.0	−9.7
MP2/cc-pVTZ[b]	0	15.7	41.3	−25.6	−23.4	−2.1
CCSD(T)/cc-pVTZ[b]	0	15.7	35.3	−27.0	−24.8	−3.2

[a] Geometries are optimized at the given level of theory, and energies are given in kcal/mol. Energies are not ZPE corrected. [b] Energy evaluated at the B3LYP/6-31G* optimized geometry

The methyl shift occurs through a transition state (**8**, Figure 7) leading from the open intermediate (**7**) to the 2-methoxy-3,3-dimethyl-2-butyl cation (**4M**, Figure 7). Table 7 lists the geometrical parameters calculated for the structures associated with the ring opening and corresponding methyl shift. Because of the steric hindrance of the methyl groups, the (*Z*)-isomer and its associated isomerization barrier were not considered for this species.

Figure 8 is a potential energy diagram of the various minima and transition states characterized on the ground state surface of $C_7H_{15}O^+$. The potential energy surface in the region appears to be relatively flat as compared to the $C_3H_7O^+$ surface. In particular, the barrier to ring opening is much smaller and is essentially identical in height to the inversion barrier at the oxygen atom. Both qualitative and quantitative differences appear when one calculates relative energies for these structures using a larger basis set and higher level of theory. As was the case for structures **1H**−**6H**, the B3LYP calculations underestimate reaction barriers for the tetramethyl species. Most notably,

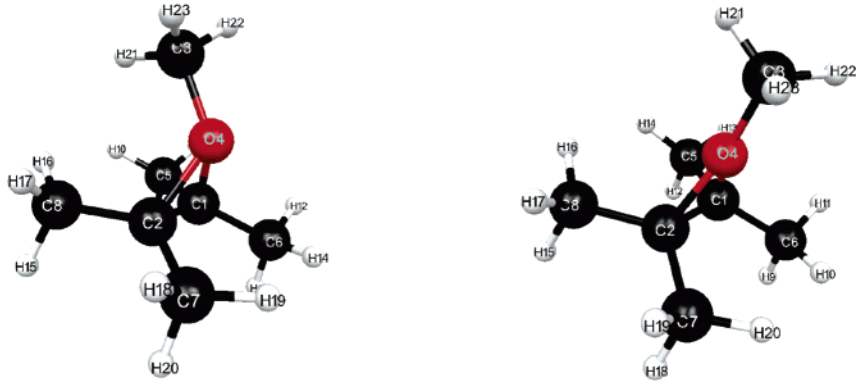

FIGURE 5. B3LYP/6-31G* geometries of the tetramethyl-substituted *O*-methylethylene oxonium ion (**1M**) and the transition state associated with inversion at the oxygen atom (**2M**).

TABLE 6. Geometrical Parameters Determined for Structures 1M and 2M at the B3LYP/6-31G* Level[a]

	C_1-C_2	C_2-O	$O-C_3$	C_2-O-C_3	$C_1-C_2-O-C_3$
1M	1.496	1.567	1.467	124.7	112.1
2M	1.530	1.503	1.471	149.3	180.0

[a] Bond lengths are given in angstroms, and bond and dihedral angles are given in degrees.

the ring-opening transition state is predicted to be significantly higher in energy than the inversion transition state at the MP2/cc-pVTZ level as opposed to the B3LYP/6-31G* calculations that determined them to be essentially identical. The B3LYP calculations also overestimate the exothermicity of the conversion of **1M** to **4M** by over 6 kcal/mol, which is relatively large since the relative energy difference at the MP2 level is only 15.5 kcal/mol. The most notable change is the relative positions of structures **7** and **8**. The relative energy of the transition state **8** is lower than the equilibrium structure **7** at the MP2/cc-pVTZ//B3LYP/6-31G* level of theory. This suggests that higher-level calculations may fail to locate either an intermediate or a transition state associated with the methyl shift from **3M** to **4M**, which is the case for the ring opening of **1H** to form **4H**.

Although quantifying solvent effects is beyond the scope of this work, an analysis of charges may lend some insight into possible solvation effects. Table 8 lists the charges on some of the heavy atoms for structures associated with ring opening in **1H** and **1M**.

Large changes are not observed in the atomic charges in going from **1H** to the transition state **3H**. There is some localization of charge on C_1 in **3H**, which would cause a greater stabilization of this structure in polar solvents as compared to **1H** and thereby lowering the activation energy. A more dramatic change is observed in going from **3H** to **4H**. The positive charge migrates from C_1 to C_2 during the hydride shift, as expected. The localization of charge on C_2 in **4H** is expected to make the ring-opening process more exothermic in polar solvents. On the basis of similar analysis of the tetramethyl analogues (Table 8), the atomic charge is more delocalized. Thus, the effect of polar solvents on the thermodynamics of the ring opening of **1M** to **4M** would be attenuated. Although analyzing charges can give a qualitative description of solvation effects, more quantitative methods (continuum[36,37] or discrete[38,39] solvent models) could be used to obtain a better understanding of the effects of solvents on this process.

Discussion

The isomerization of *O*-methylethylene oxonium (**1H**) by inversion at the oxygen atom leads to slight changes in the geometrical structure of the ion relative to the transition state (**2H**). Elongation of the C_1-C_2 bond and contraction of the epoxide C−O bonds are observed and can be understood based on changes in orbital hybridization at the oxygen atom. A similar trend is observed for the associated methylated species (**1M**). However, the bond lengths in the epoxide ring are longer in **1M**, most likely due to the steric effects of the methyl groups on the ethylene bridge. The changes in the geometries of the ring structures when traversing the ring-opening transition state are also similar between **3H** and **3M**. Significant shortening of the remaining carbon−oxygen bond from the epoxide ring (≈0.10 Å) does suggest the initial formation of a carbon−oxygen double bond. The most noticeable difference between the hydrogen containing structures and their methylated analogues is the concerted hydride shift in going from **1H** to **4H** as opposed to the stepwise methyl shift in going from **1M** to **4M** predicted by the B3LYP/6-31G* calculations. However, higher-level energy analysis suggests that the ring-opening process leading from **1M** to **4M** may be concerted. These conflicting results are reminiscent of those seen for the ring-opening process observed for **1H**, suggesting that the hydride/methyl shift occurs in a relatively flat region of the potential energy surface.

Despite being a metastable species, the *O*-methylethylene oxonium ion is relatively stable in that a significant barrier (30−40 kcal/mol) must be overcome for the structure to isomerize into a more thermodynamically favorable species. Experimental observation of this ring structure has been limited, which is not surprising given that at higher temperatures isomerization to a more stable species will become prevalent. Previous calculations[4] show that even lower energy species on the $C_3H_7O^+$ potential energy surface exist, further complicating the reversibility of the ring-opening process. While IRC calculations

(36) Tomasi, J.; Persico, M. *Chem. Rev.* **1994**, *94*, 2027−2094 and references therein.
(37) Li, J.; Hawkins, G. D.; Cramer, C. J.; Truhlar, D. G. *Chem. Phys. Lett.* **1998**, *288*, 293−298.
(38) Gao, J. *Rev. Comput. Chem.* **1996**, *7*, 119−185 and references therein.
(39) Day, P. N.; Jensen, J. H.; Gordon, M. S.; Webb, S. P.; Stevens, W. J.; Krauss, M.; Garmer, D.; Basch, H.; Cohen, D. *J. Chem. Phys.* **1996**, *105*, 1968−1986.

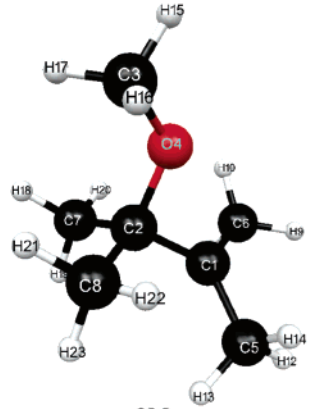

3M

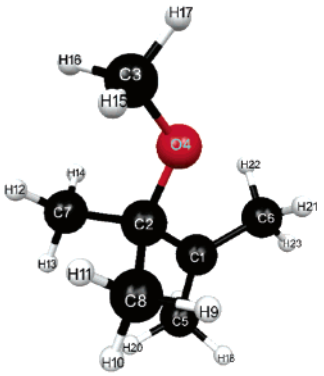

7

FIGURE 6. B3LYP/6-31G* geometries of the transition state (**3M**) associated with ring opening in **1M** and the resulting open intermediate (**7**).

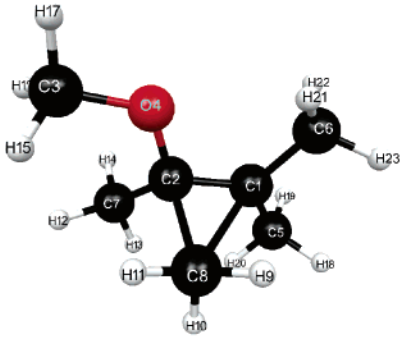

8

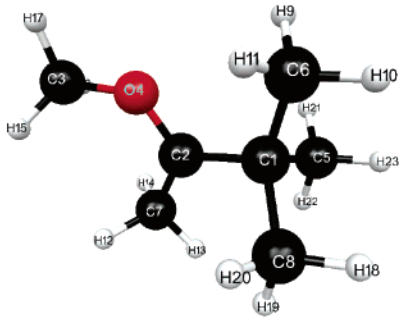

4M

FIGURE 7. B3LYP/6-31G* geometries of the 2-methoxy-3,3-dimethyl-2-butyl cation (**4M**) and the transition state structure (**8**) corresponding to methyl shift from **7**.

TABLE 7. Geometrical Parameters Determined for Structures 3M, 7, 8, and 4M at the B3LYP/6-31G* Level[a]

	C_1-C_2	C_2-O	$O-C_3$	C_1-C_2-O	C_2-O-C_3	$C_5-C_1-C_2-O$
3M	1.522	1.441	1.437	96.8	118.3	124.4
7	1.485	1.407	1.434	106.8	119.2	180.0
8	1.430	1.367	1.440	112.3	119.7	−165.8
4M	1.498	1.278	1.469	116.0	124.0	−118.3

[a] Bond lengths are given in angstroms, and bond and dihedral angles are given in degrees.

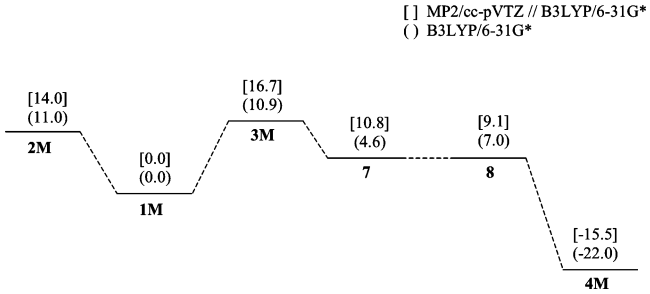

FIGURE 8. Potential energy diagram of the stationary points on the $C_7H_{15}O^+$ potential energy surface. Relative energies are in kcal/mol and are ZPE corrected.

indicate that the ring structure is connected to the *trans*-1-methoxyethyl cation (**4H**) through the previously mentioned barrier, one can see that the barrier of isomerization between the *cis*- and the *trans*-isomers is much lower in energy than the

TABLE 8. Atomic Charges Determined at the B3LYP/6-31G* Level for Structures Associated with Ring Opening of 1H and 1M[a]

	C1	C2	O	C3
1H	0.35	0.35	−0.02	0.32
3H	0.54	0.36	−0.15	0.25
4H	0.09	0.67	−0.09	0.33
1M	0.54	0.54	−0.14	0.25
3M	0.58	0.66	−0.34	0.18
4M	0.49	0.66	−0.17	0.28

[a] Hydrogen charges have been added into heavy atom charges.

ring-opening transition state. This suggests that a mixture of the *cis*- and *trans*-isomers of the 1-methoxyethyl cation would be experimentally observed upon cleavage of the ring in the *O*-methylethylene oxonium ion. However, since no other isomerization pathways associated with these species were considered, further studies would be needed to corroborate this hypothesis. The methyl-substituted analogue of **1H** is considerably less stable in that inversion at the oxygen atom is nearly isoenergetic with opening of the epoxide ring due to the significant decrease in the ring-opening barrier.

These calculations corroborate previous experimental work suggesting that the inversion of structure **1H** at the oxygen atom is the mechanism associated with coalescence of peaks in the NMR spectra. The theoretical value of 15.7 kcal/mol for the inversion barrier is reasonably close to the experimentally determined value of 10 ± 2 kcal/mol. These calculations also indicate that similar isolation of the methylated analogues would

be more difficult due to the low barrier to ring opening and subsequent methyl shift to a more stable structure.

The equilibrium structures on the oxonium ion potential surface are qualitatively similar to previous calculations of fluorine containing cations. Damrauer et al.[7] estimated that the $C_2H_4F^+$ fluoronium ion is 28.2 kcal/mol less stable than the corresponding 1-fluoroethyl cation. Our calculations predict that the *O*-methylethylene oxonium ion is higher in energy than the open structures by about the same amount of energy (25−27 kcal/mol). Alkyl shifts similar to those seen in structures **1M**−**4M** are observed in 1,2-dimethylethene and tetramethylethene bromonium ions.[12,40] Analogously, the 2-methoxyethyl cation in this study has been shown to undergo a hydride shift to the 1-methoxyethyl cation resulting in double bond character between the oxygen and the α-carbon.

Conclusion

Mechanisms associated with the isomerization of the *O*-methylethylene oxonium ion and its tetramethyl-substituted analogue have been explored using correlated electronic structure calculations. The minima and transition states associated with inversion at the oxygen atom, as well as those associated with opening of the epoxide ring, have been characterized. The calculated barrier to inversion at the oxygen atom for the *O*-methylethylene oxonium ion agrees well with the experimentally determined value. Our calculations indicate that a significantly higher barrier exists for the ring-opening mechanism that leads to more thermodynamically stable structures. This work includes the first known calculations on the *O*-methyl-2,3-dimethyl-2-butene oxonium ion along with transition states and intermediates associated with ring opening and inversion at the oxygen atom. Results show that there is a significantly lower barrier to ring opening as compared to the *O*-methylethylene oxonium ion species, leading to a lower probability of isolating this species.

(40) Hough, R. E. The Structure of Bromonium Ions and Aziridinium Imide. M.S. Thesis, Villanova University, Villanova, PA, 2005.

The effects of basis sets and correlation techniques on these ions were also analyzed in this work. Our results indicate that the B3LYP/6-31G* basis set is reliable for obtaining molecular geometries for both minima and transition states of nontrivial species such as these constrained oxonium ions. The relative energies of these systems were determined at higher levels of theory and with larger basis sets, with the MP2 calculations comparing well to CCSD(T) using the cc-pVTZ basis set. Since these methods performed well for these small systems, it is expected that a similar approach could used to accurately analyze other substituted oxonium ions. The differences observed between B3LYP and MP2 geometries for the methylated oxonium ions considered in this work are much less pronounced than those observed for protonated epoxides by Carlier and coworkers.[17] As they mention in their work, such differences are not observed when considering symmetric structures but can be quite prevalent in asymmetric structures. Despite considering asymmetric structures in this work (e.g., ring-opening transition states), we do not observe such differences. We conclude that due to the nature of these transition states (i.e., nearly complete bond breaking) for these species, one would not expect to see large differences in bond lengths using B3LYP and MP2. Despite this, future work involving similar asymmetric equilibrium structures must address differences in structures optimized at lower levels of theory (e.g., DFT and MP2).

Acknowledgment. The authors thank the Department of Chemistry and the College of Liberal Arts and Sciences at Villanova University for financial support of this research.

Supporting Information Available: Cartesian coordinates and absolute energies at the B3LYP/6-31G* level for all structures reported. This material is available free of charge via the Internet at http://pubs.acs.org.

JO0624492